The 5^{th} IVS General Meeting Proceedings, 2008, p. 53–62

Effects on the Geodetic-VLBI Observables Due to Polarization Leakage in the Receivers

Alessandra Bertarini [1], *Walter Alef* [2], *Brian Corey* [3], *Axel Nothnagel* [1], *Craig Walker* [4]

[1)] *Institute of Geodesy and Geoinformation, Bonn University, Germany*

[2)] *Max Planck Institute for Radio Astronomy, Germany*

[3)] *MIT Haystack Observatory, USA*

[4)] *National Radio Astronomy Observatory, USA*

Abstract. Polarization leakage is one of the instrumental errors that decreases the precision of the geodetic and astrometric measurements. Its effect can be corrected in the data provided one knows the leakage characteristics. In this paper we present a project to measure the polarization leakage at some geodetic VLBI stations and at the VLBA. We describe the observation strategy used to measure the leakage, the correlation process, and some preliminary results.

1. Introduction

Polarization leakage is one of the biggest of the instrumental error sources remaining in the determination of multi-band delay (MBD) and hence in the determination of geodetic and astrometric parameters such as baseline length, Earth orientation parameters, and source positions. Leakage occurs primarily due to the electrical properties and shape of the polarizer and varies with frequency. Under certain assumptions about feed performance, Rogers [1] estimates a MBD error from polarization leakage of order 14 ps. An error term this large dominates the total error from all instrumental sources [1]. Typical MBD errors from leakage are expected to be smaller than 14 ps, and indeed the few values measured to date are typically in the range 2–9 ps at 8.4 GHz (X-band) [2]. Even at this level, the leakage error is still a major contributor, if not the dominant one, to the total instrumental error in geodetic VLBI. By solving for the intrinsic source polarization during data analysis, the rss error should further improve as reported by Rogers [1].

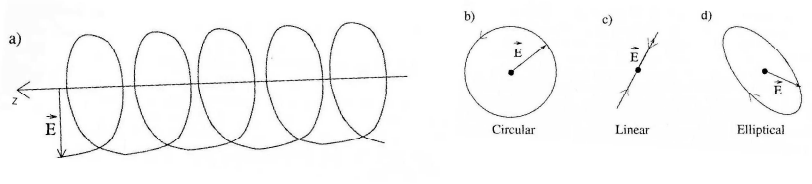

Figure 1. (a): cartoon of the electric field component of a plane monochromatic electromagnetic wave propagating along the z direction. Panels (b), (c) and (d): movement of the tip of the electric vector and representing respectively circular (b), linear (c) and elliptical (d) polarization states achieved by adjusting the phase difference between the x and y components of the wave. Taken from [5]

2. Background

2.1. Concept of Polarization

In free space, far enough from the source of the emitted radiation, an electromagnetic wave can be described as a plane propagating wave. Fig. 1a represents the projection onto two perpendicular axes, x and y, of the electric field component of a plane monochromatic electromagnetic wave propagating along the z direction.

If we consider the motion of the tip of the electric vector with time at a fixed position in space we see that the tip of $\vec{E}$ can describe a circle (Fig. 1b), a line (Fig. 1c), or an ellipse (Fig. 1d). More generally the orientation of the electric vector will change randomly with time and in this case the wave is unpolarized.

The radiation from radio astronomical sources is found to be either unpolarized or only weakly linearly polarized, which means that the radiation has either no statistical tendency or only weak statistical tendency to favour one of the two polarization states and, further, that its phase is random from one instant of time to the next.

2.2. Polarizers and Their Effects on the Geodetic Observables

VLBI, like most forms of interferometry, needs to preserve both the phase and the amplitude of the incoming radiation to perform a measurement [3]. In VLBI, the sky signal is typically collected by coupling the radiation into a waveguide through which both orthogonal polarization states can propagate. Radiation is coupled out of the waveguide into coaxial cables using electric dipole antennas, which respond to linear polarization [4]. The generally unpolarized incoming radiation (see 2.1) is a mixture of two incoherent polarization states. To maximize the signal-to-noise ratio (SNR) in the cross correlation between two antennas, one would like both antennas to select the same two

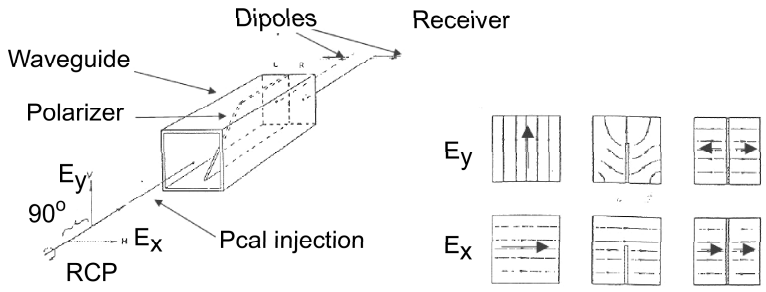

Figure 2. Left: schematic diagram of a septum polarizer. Right: the field pattern in cross section across the septum polarizer at the input, half way and at the output. Courtesy of S. Srikanth

polarization states out of the mixture. To make the selection one uses a device called a polarizer. In VLBI it is convenient to use circular polarization (CP) instead of linear polarization because the Earth is round, so antennas on different continents must point with different parallactic angles (that is the angle between the line joining the source to the north celestial pole and the line joining the source to the zenith at the antenna) and so linear feeds will not remain parallel throughout the array (unless the feeds can be rotated axially). Instead, using CP, the parallactic angle difference introduces simply a phase rotation of the fringe visibility, which can be removed in the post-correlation data analysis.

Here we describe one among the various kinds of polarizers in use in VLBI: the septum polarizer. We will, for simplicity, consider the incoming radiation as pure right circular polarization (RCP), thus having the same amplitude in the x and y directions and a 90° phase shift between the x and the y component of the wave. The wave encounters the septum polarizer, which contains a metal fin within the waveguide as shown in Fig. 2. The component of the electric field perpendicular to the fin (E_x) is divided, due to the boundary conditions on the conducting fin, in two electric field regions which have the same intensity and orientation as E_x. The component of the electric field parallel to the fin (E_y) is divided, due to the boundary conditions on the conducting fin, in two electric field regions which have the same intensity as E_y but the orientations are rotated into the horizontal plane in the clockwise direction in one region and in the counterclockwise direction in the other region. The phase velocities of the E_x and E_y components differ from each other while propagating from the polarizer input to the dipole because the septum divides the waveguide into regions that have different dimensions in the x and y directions (x is halved, y remains the same). These dimensions and the length of the septum are chosen to introduce a 90° phase shift between the E_x and E_y components. When those

fields (i.e. E_x and the rotated E_y fields with 90° phase shift) superimpose at the dipoles, they interfere constructively at one dipole and destructively at the other dipole. This logic can be repeated for pure left-circular polarization (LCP) and the output power will appear at the other dipole. The general case is a mixture of RCP and LCP input, which will be separated to produce outputs on both dipoles. In the real case, a band of frequencies is observed and the theoretical phase difference inserted by the polarizer between the two linear polarizations measured at one dipole output is an accurate 90° only at two frequencies. In this broad-band case, the septum polarizer will not separate the two polarization with perfect purity at most frequencies and some contamination from the unwanted polarization will add algebraically to the signal.

The effect of leakage is to perturb the visibility phase in one polarization with a small amount of signal leaking from the other polarization. The leakage and hence the phase perturbation is frequency dependent and so perturbs the delay and will not close around a triangle of baselines [8, 9].

2.3. Past Studies

That polarization leakage affects the VLBI measurements has been known for more than a decade and both the geodetic and astronomical communities have conducted some studies to either estimate or quantify the contamination of the observables due to the polarization leakage. Rogers [1] adopted a nominal value for polarization leakage of −15 dB (corresponding to a leakage of about 3% of the power from one polarization into the other) and estimated from it, for unpolarized radio sources, a MBD error of the order of 14 ps (4.2 mm) or less and for 10% polarized radio sources typically an extra 8 ps (2.4 mm) error assuming that the polarization leakage introduces a phase gradient over 360 MHz bandwidth. Corey & Titus [2] found that the VLBA antennas polarization leakage is less than −20 dB at 2.3 GHz (S-band) and 8.4 GHz (X-band), so the leakage is less than 1% of the power from one polarization into the other, and estimated from that a maximum of 1.0 ps (0.3 mm) MBD error at X-band and a maximum of 2.2 ps (0.7 mm) MBD error at S-band. At the geodetic sites, Corey & Titus [2] measured the polarization leakage to be typically greater than −20 dB, leading to MBD errors between 2 ps (0.6 mm) and 9 ps (2.7 mm) at X-band.

The variation of leakage amplitude with frequency has been measured for the European VLBI Network antennas by Massi et al. [9]. This amplitude change causes lower dynamic range (peak to rms ratio) in images made using these antennas compared to images made using the VLBA antennas.

The need for new measurements arose because in the previous studies only approximate values were established: the calibrators were assumed to be unpolarized, the sources were not imaged, the bandwidth spanned for the geodetic antennas was only 360 MHz of the 720 MHz available at X-band [2], and some stations upgraded the receivers since those measurements were made.

3. The New Project

In our study we assume that the observed sources can be polarized, therefore we will image them to determine the source structure and intrinsic polarization simultaneously with the leakage determination. We spanned the so called geodetic wide band that is from 8212 MHz to 8932 MHz at X-band and from 2225 MHZ to 2365 MHz at S-band. We will also measure the polarization leakage every 8 MHz for better interpolation of the leakage vectors across the whole bands and in case the geodetic frequency sequence is changed in the future. This study could be considered as a pilot project to establish the procedure for high quality measurements and corrections of the leakage. It is based upon a subset of antennas and later could be expanded to the whole geodetic network.

3.1. Strategy

Leakage is detected by the following procedure. In the absence of leakage the signals received in the LCP channel and RCP channel are uncorrelated gaussian noise processes and cross correlation between them will yield no coherence. If leakage is present then some of the signal in one polarization channel will add to the signal in the other polarization channel. By cross-correlating the contaminated RCP channel at one antenna and the contaminated LCP channel at the other antenna one will find coherence caused by the LCP in the LCP channel correlating against the LCP that leaked into the RCP channel. Geodetic stations mostly have only RCP, but measurements of the leakage for these stations are still possible if the antenna at the other end of the baseline has dual-polarization receivers. Therefore, we used the 10 VLBA antennas for their dual polarization capability plus 10 geodetic antennas. Correlation was performed between all possible combination of polarization (i.e. RCP against RCP, LCP against LCP, RCP against LCP and LCP against RCP). Data reduction is proceeding using AIPS (Astronomical Image Processing System), which is one of the most widely used interferometric data reduction packages for radio astronomy. In AIPS we measure the terms that represent the leakage, which in jargon are called D-terms ([5, 6]). Once the D-terms are available we will modify the post-correlator software to use the D-terms to correct the effects of the leakage and will perform validation tests.

3.2. Scheduling

To cover from 8212 MHz to 8932 MHz completely requires 720 MHz divided into 8 MHz per VC/BBC sideband, i.e. 15 setups observing three frequencies in X-band and one frequency in S-band simultaneously.

The production of the schedule file was made quite complicated by some tuning and patching constraints at both the VLBA and geodetic antennas. Whilst the geodetic stations have 14 video converters (VC), the VLBA antennas are limited to eight baseband converters (BBC) and we have paired those to

get both hands of polarization. Instead of using only four VCs at the geodetic stations, since they can observe only RCP, we used all 14 for simplicity of scheduling, providing redundant frequency coverage as backup in the case of a VC problem, though with the risk of increased crosstalk between VCs when many are set to the same local oscillator (LO) setting. The dichroic mirror that enables simultaneous S-band and X-band observing at the VLBA stations remains deployed only when at least one BBC is tuned to X-band and at least one BBC is tuned to S-band. Thus, we needed to observe with at least one BBC in each band at all times. The Mark IV data acquisition racks have three intermediate frequency (IF) inputs, each with their own band-limiting filters [12] that leave a gap between 8580 MHz and 8680 MHz that cannot be observed. To ease the work at the Mark IV stations we kept the standard geodetic patching, reducing the probability of false patching and consequent loss of one or more frequency setups, though increasing the complexity of the scheduling as described above.

We had 24 h of observing time on the IVS and VLBA antennas. We observed the first 12 h at 512 Mbps with 2 bit sampling switching among the 15 frequency setups. The second 12 h were observed using the rapid (R1) frequencies at 256 Mbps, 1 bit sampling switching among four frequency setups.

Target sources were OQ 208 and 3C 84 as they are known to be nearly unpolarized. We observed also some backup sources for calculating the polarization leakage and as calibrators.

3.3. Correlation

Correlation of the experiment started in October 2007 using the Bonn MPIfR/BKG Mark IV correlator and produced fringes to all the VLBA antennas except Hancock, which was down during the observation, and to most of the geodetic antennas. Unfortunately we lost Ny Alesund, due to manpower limitations and Kokee Park and Fortaleza due to technical reasons. Since the correlator has eight Mark 5A playback units and we had a total of 16 stations, we ran the correlation in six passes to form all the baselines. In December 2007 we fringe fitted and checked the quality of the data using the HOPS (Haystack Observatory Postprocessing System) package and found that most setups yielded good quality data but some were degraded by RFI, especially in S-band. One setup might require recorrelation due to a problem encountered in fringe fitting the data.

3.4. Data Reduction

Data reduction in AIPS started in January 2008. We reduced the data for the first frequency setup in S-band (i.e. 2225 MHz). The results are still preliminary and the setup will soon be reprocessed to understand some unresolved issues. For clarity we will present the data reduction step by step.

The data were imported into AIPS and a priori amplitude calibration was

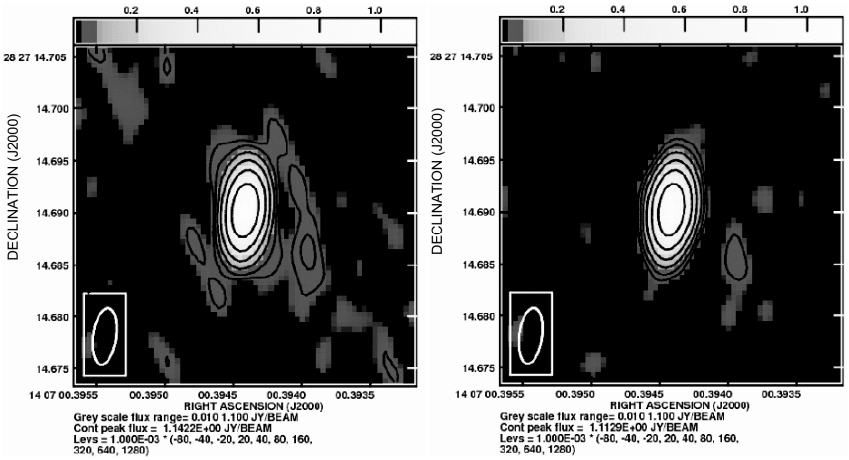

Figure 3. Image of OQ 208 at 2225 MHz with the VLBA and geodetic array with phase self calibration (left) and after amplitude self calibration (right)

performed based on the system temperature ($T_{\rm SYS}$) and antenna sensitivity measured at the stations. The conversion factor between correlator amplitude and flux density in Jy is derived from $T_{\rm SYS}$ measurements in each polarization and the knowledge of the sensitivity of the antennas, possibly as a function of elevation for each polarization. The a priori amplitude calibration contained large systematic errors because the purely geodetic stations did not provide the elevation-dependent gain curves and many did not provide the system equivalent flux density (SEFD) and its variation with frequency. The remaining amplitude calibration errors could be corrected later by applying amplitude self calibration after imaging the source.

After a priori amplitude calibration we performed phase, delay and delay-rate calibration by fringe fitting the parallel hands of polarization (RCP-RCP and LCP-LCP) in AIPS.

The AIPS fringe fit algorithm is global, i.e. it uses constraints from all baselines to an antenna when determining a delay solution for that antenna and potentially gives better SNR compared to the baseline-based fringe fit algorithm used by HOPS.

After fringe fitting, we applied bandpass calibration for compensating the gain variation with frequency and to enable extraction of more than one leakage term within the 8 MHz bandwidth per BBC/VC.

To reduce further the calibration errors in phase and amplitude, we iteratively improved our model of the sky brightness distribution using self calibration [10]. Fig. 3 shows the before-and-after images after two cycles of phase self calibration and one of amplitude self calibration. The artifacts in the image were reduced by the improvement in the amplitude calibration.

At this point the total intensity calibration was complete and the polariza-

tion calibration began. The first step was to correct the delay offset between the two opposite hands of polarization due to differences in the electronic path length before calculating the leakage. The cross-hand (RCP-LCP and LCP-RCP) delay offset following the parallel hand fringe fit is the same for all the antennas since much of the antenna-based delay differences gets absorbed into the parallel hands delay solutions. Thus cross-hand fringe fit was performed between only two VLBA antennas. The cross-hand delays and phases were averaged to improve SNR, allowing for their sign inversion when the polarizations are swapped [13]. This procedure ties the RCP and LCP channels at all antennas, including the geodetic antennas although they have no LCP channels.

The derivation of leakage proceeded as follows. If the source is polarized, the LCP-RCP (and RCP-LCP) cross correlations are non zero. The RCP-LCP and LCP-RCP cross correlations contain also a contribution due to leakage between the polarization channels. The two contributions can be separated since the LCP-RCP phase due to source polarization rotates with the parallactic angle whereas the LCP-RCP phase due to leakage remains constant throughout an observation (and over much larger periods) [5]. This principle is illustrated in Fig. 4, which shows the LCP-RCP cross correlation real and imaginary components for OQ 208 throughout the observation. The data were corrected for the parallactic angle, which means that the visibility phases were rotated according to the parallactic angle, causing the LCP-RCP phase due to source polarization to remain constant and the LCP-RCP phase due to the leakage to rotate. Since OQ 208 is unpolarized, we see the rotating leakage vector centered at zero in the real/imaginary plane as shown in the left most two panels of Fig. 4. After deriving the D-terms and correcting the data for their effect, the leakage disappears as shown in the right most two panels of Fig. 4.

The amplitude of the leakage term in this first setup was found to vary from -40 dB (1% of voltage leakage of one polarization into the other) at Wettzell to -15 dB (17% of voltage leakage) at Westford. We checked with the HOPS package whether we could detect the signal produced by the leakage in the cross-correlation of the left circular feed at one VLBA antenna and the right circular feed at the Westford antenna and indeed had a detection.

The large leakage values derived above need not yet be of concern, since this analysis represents only one channel that lies at extreme edge of the band where the worst leakage is expected. The concern for the geodesist lies in the variation with frequency of both the phase and amplitude of the leakage. Additionally, geodesy is interested in the leakage correction to the parallel hands (i.e. RCP-RCP) whilst astronomy is not, since the contribution is small enough to be ignored for continuum imaging purposes. AIPS does not perform the parallel-hand correction, therefore we had to calculate it ourselves. We found that the leakage causes a difference in amplitude, ΔA, of 0.016 Jy and a difference in phase, $\Delta\phi$, of 1° for the baseline Pie-Town - Westford and source OQ 208 with 1.33 Jy in the the S-band channel we analyzed. If phase is constant across the 140 MHz band, then $\Delta\phi = 0$ and so $\Delta\tau = 0$, i.e. no change in delay would be

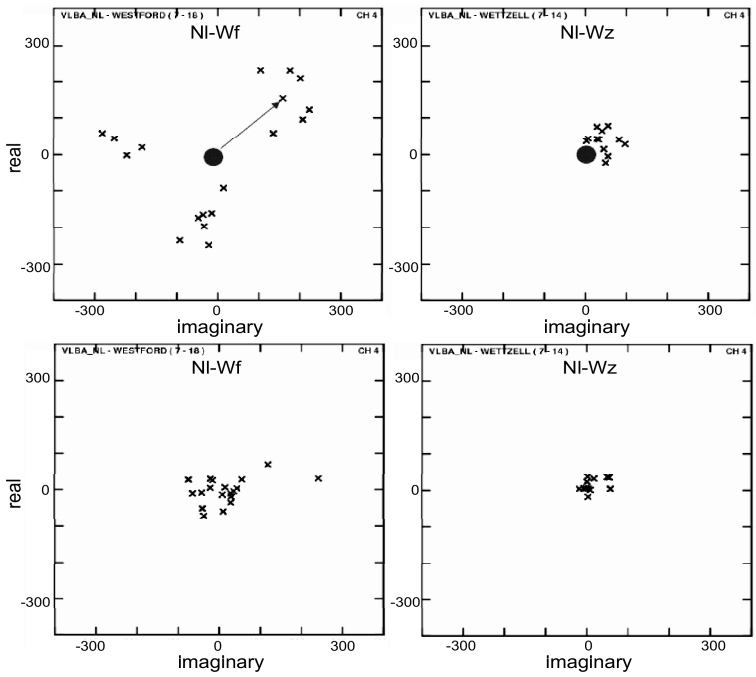

Figure 4. LCP-RCP visibility on the unpolarized source OQ 208 plotted in the imaginary vs real plane for the baseline North Liberty - Westford (first and third panels) and the baseline North Liberty - Wettzell (second and fourth panels). Visibilities are shown before (first and second panels) and after (third and fourth panel) the corrections for the instrumental polarization were applied. The big dot at the center of the images in the first and second panels is the origin of the axes and the crosses are the measured visibilities, which are seen to rotate due to the leakage vector. For clarity one of the vectors has been drawn in full for the baseline North Liberty - Westford. Third and fourth panels: same as first and second panels, but after having the D-term correction applied. The residual leakage vector has almost zero amplitude

caused by the polarization leakage. From the previous studies we know that this is not the case and if we assume a change of visibility phase of 2° across 140 MHz at S-band, then we have a change in delay of 37 ps (11 mm).

The data reduction for the other 14 frequency setups observed in the first 12 h and four setups observed in the second 12 h will lead to the measurement of the rate of change of the leakage phase across the bands.

The change of the leakage phase across the bands is not expected to change with time. Gomez et al. [11] found the leakage to be stable over a period of 1.3 years. Further, data from some VLBA monitoring programmes suggest that the leakages do not change much, unless station hardware is changed [11].

4. Summary

The polarization leakage is one of the major instrumental sources of error, is unavoidable and is frequency dependent since it occurs due to the electrical properties and shape of the polarizer. It cannot be absorbed in the clock model since it is baseline based and therefore it contaminates the delay measurements. The correction will yield a better accuracy of the delay observables and, thus, of the geodetic and astrometric parameters.

Acknowledgements

We thank Alan Roy for helping throughout the proposal, scheduling and data reduction.

References

[1] Rogers, A.E.E. Instrumentation Improvements to Achieve Millimeter Accuracy. Proceedings of the AGU Chapman Conference on Geodetic VLBI: Monitoring Global Change, NOAA Technical Report NOS 137, NGS 49, 1–6.

[2] Corey, B., M. Titus. Antenna Cross-Polarization Characteristics at Geodetic VLBI Stations. 4th IVS General Meeting Proceedings. Behrend, D. and Baver, K.D. (eds.), 2006.

[3] Thompson, A.R., J.M. Moran, G.W. Swenson. Interferometry and Synthesis in Radio Astronomy. John Wiley & Sons, Inc. (eds.), 2001.

[4] Hertz, H. Ueber Strahlen Electrischer Kraft Annalen der Physik und Chemie v. 36, Issue 4, 769–783, 1889.

[5] Cotton, W.D. Polarization in Interferometry. Synthesis Imaging in Radio Astronomy II. Taylor, G.B., Carilli, C.L., Perley, R.A. (eds.), 1999, 111–126.

[6] Sault, R.J., T.J. Cornwell. Hamaker-Bregman-Sault Measurement Equation. Synthesis Imaging in Radio Astronomy II. Taylor, G.B., Carilli, C.L., Perley, R.A. (eds.), 1999, 111–126.

[7] Rohlfs, K., T.L. Wilson. Tools of Radio Astronomy. Springer (eds.), 2004.

[8] Massi, M., S. Aaron. Stability of EVN D-terms, EVN Doc No 77., 1997.

[9] Massi, M., M. Rioja, D. Gabuzda, et al. Baseline errors in European VLBI Network measurements III. The dominant effect of instrumental polarization. Astron. Astrophys., v. 318, L32, 1997.

[10] Cornwell, T., E.B. Fomalont. Self-Calibration. Synthesis Imaging in Radio Astronomy II. Taylor, G.B., Carilli, C.L., Perley, R.A. (eds.), 1999, 187–199.

[11] Gomez, J.L., A.P. Marscher, A. Alberdi, et al. Polarization calibration of the VLBA using the D-terms. VLBA Scientific Memo No 30, 2002.

[12] Clark, T.A., A.E.E. Rogers. Mark III VLBI Data Acquisition Terminal. GSFC, NASA, 1982.

[13] Kemball, A.J. VLBI Polarimetry. Synthesis Imaging in Radio Astronomy II. Taylor, G.B., Carilli, C.L., Perley, R.A. (eds.), 1999, 187–199.